

Dissociative recombination and excitation of H_2O^+ and HDO^+

M. J. Jensen, R. C. Bilodeau,* O. Heber,† H. B. Pedersen, C. P. Safvan, X. Urbain,‡ D. Zajfman,† and L. H. Andersen
Institute of Physics and Astronomy, University of Aarhus, DK-8000 Århus C, Denmark

(Received 7 April 1999)

Dissociative recombination and excitation of H_2O^+ and HDO^+ in the vibrational ground state have been studied at the heavy-ion storage ring ASTRID. Absolute cross sections have been measured in the energy range from ~ 0.1 meV to ~ 50 eV. The total cross sections for dissociative recombination are essentially the same for the two molecular ions. Complete branching ratios for all possible product channels in dissociative recombination at $E=0$ have been determined. Three-particle breakup accounts for $\sim 60\%$ of the recombination events. With HDO^+ , recombination into $\text{OD}+\text{H}$ is twice as probable as recombination into $\text{OH}+\text{D}$. An isotope effect is also evident in the cross sections for dissociative excitation of HDO^+ , where H^+ production is more likely than D^+ production. [S1050-2947(99)01910-1]

PACS number(s): 34.80.Ht, 34.80.Lx

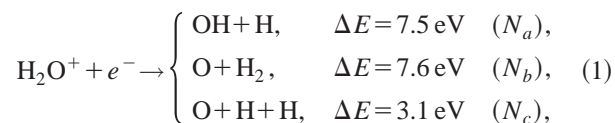
I. INTRODUCTION

Dissociative recombination (DR) is the reaction in which a positively charged molecular ion recombines with an electron and dissociates into neutral fragments. DR of polyatomic molecular ions has attracted a great deal of interest, because of its importance for the chemistry of interstellar clouds [1]. Knowledge about absolute cross sections and branching ratios is vital for the modeling of these environments. Dissociative excitation (DE) is the process in which an incoming electron excites and dissociates the molecular ion without being bound to any fragment in the final state. This process is normally not energetically allowed at low energy, but is important for collisions energies in the region ≥ 10 eV, and is consequently a topic of interest when considering plasmas at relatively high temperatures. From a more fundamental point of view, DR and DE experiments may provide information about highly excited electronic states and dissociation pathways, which is complementary to what can be obtained from photodissociation experiments.

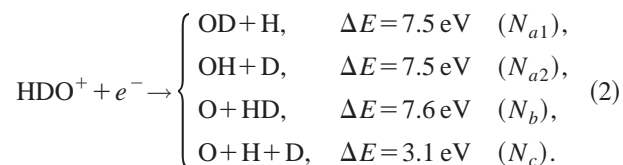
Various experimental techniques have been used to obtain cross sections and branching ratios for DR and DE. Traditionally, single-pass merged or crossed beam experiments and plasma-afterglow experiments have dominated the field. However, in recent years, storage rings have proven to be a valuable tool for studying in particular dissociative recombination, and several polyatomic molecular ions have been studied using the storage ring technique [2–9]. The long storage time allows infrared active vibrational modes to relax to the ground state, producing a better defined target than in single-pass experiments. The high storage energy (\sim MeV) simplifies the detection of reaction products compared to that of flowing-afterglow experiments, where the reactions take

place in a plasma, and hence products are more difficult to identify.

In the present paper, we report on DR and DE of H_2O^+ and HDO^+ . Three dissociation channels are energetically allowed in the dissociative recombination of H_2O^+ with electrons at relative energy $E=0$:



where ΔE is the energy release for production of ground-state products [10,11] and N_i are the branching ratios. Correspondingly, in the case of HDO^+ , the following four dissociation channels are energetically allowed:



Previously, a number of studies have been conducted on the DR of H_2O^+ . In 1983, Mul *et al.* measured the absolute cross section for DR of H_2O^+ in the energy range 0.005–1 eV [12]. A few years later, Rowe *et al.* performed the first branching ratio measurement with H_2O^+ in a flowing-afterglow experiment [13]. The branching ratios were measured again recently by Vejby-Christensen *et al.* [7] at the ASTRID storage ring, where also the present experiment was conducted. General theories predicting branching ratios for DR of polyatomic molecules have proven difficult to develop. Attempts have been made by Bates [14,15] and Herbst [16]. However, Bates was unable to obtain agreement with experiments, and the theory of Herbst was concluded to possess no predictive power, even though the model was modified in order to match experimental results for a number of systems [17].

We present here measurements of the DR and DE of HDO^+ , and accordingly a study of isotope effects in the DR and DE of water. Hydrogen exchange reactions have become

*Present address: Department of Physics and Astronomy, McMaster University, Hamilton, Ontario, Canada L8S 4M1.

†Permanent address: Department of Particle Physics, Weizmann Institute of Science, Rehovot, 76100, Israel.

‡Permanent address: Département de Physique, Université Catholique de Louvain, B1348, Louvain-la-Neuve, Belgium.

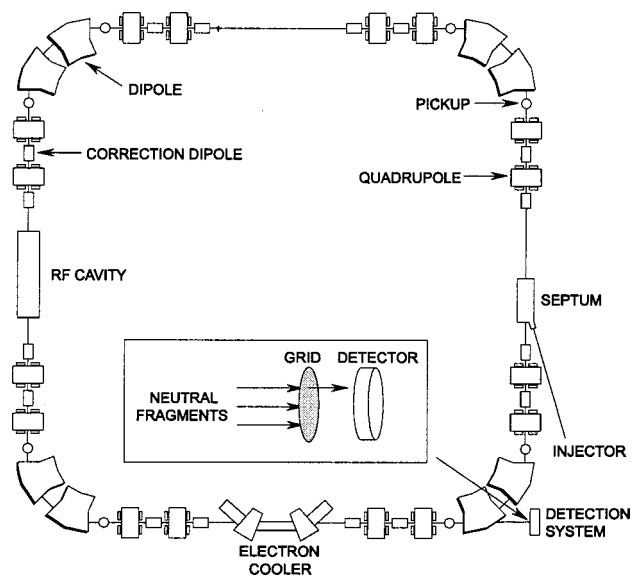


FIG. 1. Schematic diagram of the ASTRID storage ring. The inset shows a close-up on the detector region.

important for studying protein structure, stability, and dynamics [18]. In such experiments, hydrogen and deuterium are exchanged between NH groups of a peptide or protein and solvent hydrogens from H_2O and D_2O . The present study involves a controlled study of OH and OD bond breaking in water molecules and may eventually be of help in understanding more complex isotope effects in complex biological systems. Isotope effects in DR have been studied in a few other systems. Tanabe *et al.* have compared cross sections for DR of HeH^+ and HeD^+ [19], and several authors have studied isotope effects in the DR of H_3^+ [4,5,20–23]. In the case of water, isotope effects have been studied in a variety of other fragmentation processes. Photodissociation of HDO has received special attention [24–33], but also bimolecular reactions [34], electron-impact dissociation [35], and the decay of the doubly charged water ion [36] have been studied.

II. EXPERIMENT

The present experiment was carried out at the heavy-ion storage ring ASTRID in Aarhus, Denmark (see Fig. 1). H_2O^+ ions were produced in a radio-frequency (RF) ion source from H_2O vapor. Two different methods were used in the production of HDO^+ . The ions were produced in an electron-impact ion source [37] from D_2O vapor and H_2 gas for the cross-section measurements, and in an RF ion source from vapor from a mixture of H_2O and D_2O for the branching ratio measurements. After preacceleration to 150 keV, the ions were injected into the ring and by means of a radio-frequency system further accelerated to 6 MeV. The average pressure in the ring was $\sim(3-5) \times 10^{-11}$ mbar, which resulted in a storage lifetime of ~ 4 s for both H_2O^+ and HDO^+ . After reaching the final storage energy, the ion beams were merged with an essentially monoenergetic electron beam provided by the electron cooler. The electron cooler is described elsewhere [38,39]. Since all vibrational modes in H_2O^+ and HDO^+ are infrared active, the 6-s-long acceleration period allowed the ions to decay to their vibra-

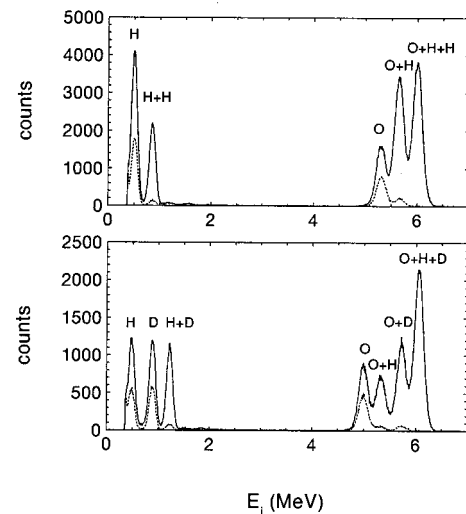


FIG. 2. Energy spectra for H_2O^+ and HDO^+ with electrons (full curves) and without electrons (dashed curves), measured at $E=0$ with the 70% transmission grid in front of the detector.

tional ground state before the data taking starts.

A. Cross sections

DR and DE cross sections as a function of relative energy were measured by varying the electron energy. The relative energy E is related to the electron and ion energies in the laboratory frame, E_e and E_i , through the equation

$$E = \frac{1}{2} m_e (v_i - v_e)^2 = \left[\left(\frac{m_e}{M_i} \right) \sqrt{E_i} - \sqrt{E_e} \right]^2, \quad (3)$$

where M_i is the ion mass, m_e is the electron mass, and v_i and v_e are the corresponding velocities.

Neutral particles produced by DR and DE in the electron beam (or by collisions with the residual gas) were detected by an energy-sensitive 60×40 mm² surface-barrier detector located 6 m downstream, behind the dipole magnet following the electron cooler (see Fig. 1). This detector enabled separation between DR and DE events. After dissociation, each fragment carries an energy proportional to its mass. Since neutrals produced in one event hit the detector essentially simultaneously, a DR event will always deposit the full beam energy E_0 in the detector, whereas a DE event will deposit only a fraction of E_0 , corresponding to the fraction of the total mass carried by the neutral fragments. In the H_2O^+ case, for example, the DE channel leading to OH and H^+ will contribute to a peak at $\frac{17}{18} E_0$, and the DE channel leading to O and H_2^+ will contribute to a peak at $\frac{16}{18} E_0$, etc. (see Fig. 2).

In order to subtract background (neutrals produced by collisions with the residual gas), the electron beam was turned on and off (chopped) at a frequency of 20 Hz. The absolute rate coefficient for a given channel in terms of measurable quantities is then given by

$$\langle v\sigma \rangle = \frac{N_s - N_b}{N_{\text{ion}}} \frac{v_i}{n_e \Delta L \epsilon}, \quad (4)$$

where v is the relative velocity, σ the cross section, v_i the ion velocity, n_e the electron density, ΔL ($= 0.85$ m) the length of the electron cooler, and ϵ ($= 1$) the detection efficiency. N_s and N_b are the rates of neutrals in the given energy window on the detector measured with the electron beam on and off, respectively. N_{ion} is the flux of ions through the electron cooler. The ion-beam current was measured by a beam current transformer capable of measuring bunched ion-beam currents down to 10–50 nA.

Relative rate coefficients as a function of energy were obtained by normalizing the signal to the rate of neutrals N_0 in a given energy window produced from collision with the residual gas, i.e., measured when the electron beam was off,

$$\langle v\sigma \rangle_{\text{relative}} = \frac{N_s - N_b}{N_0 n_e}. \quad (5)$$

Relative rate coefficients were put on an absolute scale using Eq. (4) at a single relative energy.

When extracting cross sections from the measured rate coefficients, the electron velocity distribution must be taken into account. The rate coefficient is the velocity-weighted cross section averaged over the electron velocity distribution $f(\mathbf{v})$ in the rest frame of the ions:

$$\langle v\sigma \rangle = \int v\sigma(v)f(\mathbf{v})d\mathbf{v}. \quad (6)$$

$f(\mathbf{v})$ is given by the flattened Maxwell function

$$f(\mathbf{v}) = \frac{m_e}{2\pi kT_{\perp}} e^{-m_e v_{\perp}^2/2kT_{\perp}} \sqrt{\frac{m_e}{2\pi kT_{\parallel}}} e^{-m_e(v_{\parallel}-\Delta)^2/2kT_{\parallel}}, \quad (7)$$

where v_{\perp} and v_{\parallel} are the relative electron velocities perpendicular and parallel to the ion-beam direction, and $\Delta = |v_i - v_e|$ is the detuning velocity between electrons and ions [38]. In the present experiment, the electron beam was adiabatically expanded in a magnetic field decreasing by a factor of 4.5 [40]. The resulting temperatures were expected to be $kT_{\perp} \approx 25$ meV and $kT_{\parallel} \approx 0.5$ meV.

Throughout this paper, cross sections are defined as $\langle \sigma \rangle = \langle v\sigma \rangle / \Delta$. A significant deviation from the true cross section will occur only at low energy ($E \lesssim kT_{\perp}$) where the electrons have velocities deviating from Δ .

The measured cross sections consist of contributions from the central region of the cooler where the electron and ion velocities are parallel, and from the toroid regions where the electron and ion beams merge and separate. In the central region, the relative energy is well defined, whereas in the toroid regions a range of larger relative energies is encountered. The measured rate coefficient at a given energy therefore contains contributions from higher energies. These contributions can be calculated and subtracted using the measured rate coefficients. The cross sections presented in this paper were corrected for these toroid contributions.

B. DR branching ratios

Branching ratios at cooling were obtained using the energy spectra from the energy-sensitive surface barrier detector mentioned in Sec. II A. The electron beam was also in

this case chopped in order to allow for proper background subtraction. At $E=0$, only DR channels are open, thus the energy spectrum will, after background subtraction, in principle consist of a single peak at the full beam energy E_0 . In order to separate the different DR channels, a grid with a finite transmission T was inserted in front of the detector (see Fig. 1). This method has been used in a number of DR experiments [2–7]. The present measurements were performed with two different grids, $T_1 \approx 25\%$ and $T_2 \approx 70\%$.

Particles stopped by the grid will not contribute to the signal, and the original peak due to DR at E_0 will split up into a series of peaks as shown in Fig. 2. Branching ratios can then be obtained since the probability for one particle to be transmitted is T , whereas two and three particles will be transmitted with probabilities T^2 and T^3 , respectively. As an example, the a channel in the DR of H_2O^+ contributes to the E_0 peak with probability T^2 , to the $\frac{17}{18}E_0$ peak with probability $T(1-T)$, and to the $\frac{1}{18}E_0$ peak with probability $T(1-T)$. A set of equations connecting the counts in each energy peak to the number of events n_i in each DR channel can be set up. In the case of H_2O^+ , the equations read

$$\begin{pmatrix} N(\text{O}+2\text{H}) \\ N(\text{O}+\text{H}) \\ N(\text{O}) \\ N(2\text{H}) \\ N(\text{H}) \end{pmatrix} = \mathbf{T}_{\text{H}_2\text{O}} \begin{pmatrix} n_a \\ n_b \\ n_c \end{pmatrix}, \quad (8)$$

where

$$\mathbf{T}_{\text{H}_2\text{O}} = \begin{pmatrix} T^2 & T^2 & T^3 \\ T(1-T) & 0 & 2T^2(1-T) \\ 0 & T(1-T) & T(1-T)^2 \\ 0 & T(1-T) & T^2(1-T) \\ T(1-T) & 0 & 2T(1-T)^2 \end{pmatrix}. \quad (9)$$

A similar set of equations was used for HDO^+ .

In the analysis, we introduced two different transmission coefficients, T_h for heavy particles (O and heavier) and T_l for light particles (HD and lighter). With the geometry of our experiment, a minor fraction of the light particles (H, D, and H_2) produced in the two-particle breakup channels missed the detector. The loss coefficients were determined from the spectra taken without a grid in front of the detector. In these spectra, loss of light particles was responsible for peaks at fractions of E_0 , and the loss coefficients were obtained from a comparison of the count numbers in these peaks with the count number in the E_0 peak. With these modifications, we obtain five equations with five unknowns [T_l , T_h , and n_i ($i=a,b,c$)] in the case of H_2O^+ , and seven equations with six unknowns in the case of HDO^+ .

The equations were solved numerically, utilizing a χ^2 minimization, yielding T_l , T_h , and n_i . Branching ratios were obtained after normalization:

$$N_i = n_i / \sum_k n_k. \quad (10)$$

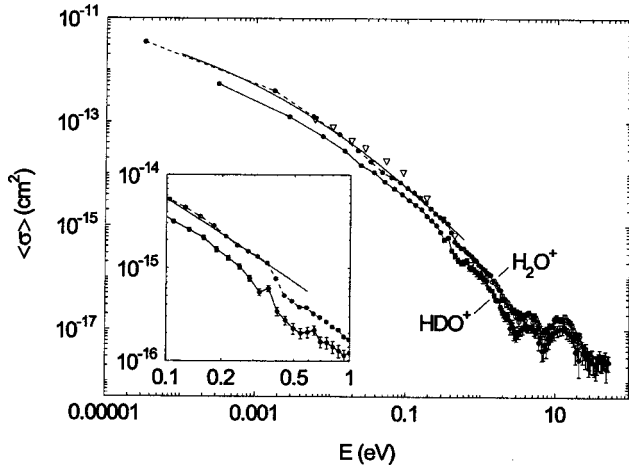


FIG. 3. Cross sections for DR of H_2O^+ (\circ , dashed line) and HDO^+ (\bullet , solid line) as a function of energy, error bars representing the uncertainty in the relative measurement. The full curve shows $\langle\sigma\rangle = \langle v\sigma\rangle/\Delta$ calculated for $\sigma \propto E^{-1.35}$. The H_2O^+ results of Mul *et al.* [12] are shown as ∇ . A close-up on the region around 0.3 eV is shown in the inset.

III. RESULTS AND DISCUSSION

A. DR cross sections

Cross sections for dissociative recombination of H_2O^+ and HDO^+ are shown in Fig. 3. The uncertainty associated with the absolute measurement, mainly due to the uncertainty in the ion-beam current measurement, is $\pm 25\%$ for H_2O^+ and $\pm 45\%$ for HDO^+ . Earlier H_2O^+ results obtained from a single-pass merged beam experiment performed by Mul *et al.* [12] are plotted for comparison. The two H_2O^+ cross sections are in good agreement.

Rate coefficients at $T=300$ K are extracted from the present measurements by integrating the cross sections in accordance with the equation [12]

$$\alpha(T) = \frac{8\pi m_e}{(2\pi m_e kT)^{3/2}} \int_0^\infty \sigma(E) e^{-E/kT} E dE, \quad (11)$$

yielding

$$\alpha(300\text{ K}) = \begin{cases} (2.6 \pm 0.7) \times 10^{-7} \text{ cm}^3/\text{s}, & \text{H}_2\text{O}^+, \\ (1.5 \pm 0.7) \times 10^{-7} \text{ cm}^3/\text{s}, & \text{HDO}^+. \end{cases} \quad (12)$$

Our measurements reveal a marked resemblance between H_2O^+ and HDO^+ concerning the energy dependence of the cross sections, showing no visible isotope effects. This deviates from the behavior observed in similar experiments with H_3^+ and the corresponding isotopically substituted molecules H_2D^+ , HD_2^+ , and D_3^+ [4,5,20–23]. The DR cross sections for HeH^+ and HeD^+ also show different energy dependences [19]. In the present experiment, no such effects were observed. On the absolute scale, the cross sections for H_2O^+ and HDO^+ are identical within the uncertainties, although we cannot exclude a possible isotope effect.

The DR cross sections decrease monotonically at energies lower than ~ 2 eV. This decrease is significantly faster than the E^{-1} behavior expected for the “direct” process, which may indicate that “indirect” processes involving vibra-

TABLE I. Vibrational excitation energies in eV, extracted from molecular constants given in [50].

Mode	H_2O^+	HDO^+
(010)	0.175	0.154
(020)	0.345	0.305
(100)	0.398	0.295
(001)	0.403	0.400

tionally excited Rydberg states are important [41,42]. In Fig. 3, a cross section $\sigma \propto E^{-1.35}$ convoluted with our experimental electron velocity distribution in accordance with the equation $\langle\sigma\rangle = \langle v\sigma\rangle/\Delta$ is demonstrated to fit the measured cross sections up to ~ 0.3 eV.

In the energy region 0.3–0.4 eV, the cross section drops by a factor of 3 approximately (shown in the inset in Fig. 3). No new electronic states appear at this energy, and the feature must therefore be related to the nuclear motion. The drop is clearly too abrupt to be accounted for by a change in some Franck-Condon overlap. Instead, we suggest that the drop is caused by the opening of a new autoionization channel of the neutral system (formed by electron capture) into a vibrationally excited state of the ion. Such a process will compete with DR and act as a depletion mechanism. Thresholds for vibrational excitation are given in Table I. For both H_2O^+ and HDO^+ , the drop coincides with thresholds for excitation of the symmetric (100) and antisymmetric (001) stretching modes. The thresholds for excitation of the bending mode (010), on the other hand, appear at lower energies but cannot be associated with any clear features in the cross sections. Assuming the branching ratios measured at $E=0$ eV to be roughly valid at energies up to ~ 0.5 eV, the DR process is seen to proceed mainly through the *a* and *c* channels (see Sec. III C). The nuclear motion associated with these channels is expected to have a more favorable Franck-Condon overlap with the excited stretching states than the excited bending states. Therefore, the depletion mechanism suggested here will be of considerable importance only in connection with the stretching modes as observed in the experiment.

Two pronounced peaks appear around 5 eV and 15 eV, respectively. These structures can be attributed to electron capture to Rydberg states converging to electronically excited states of the molecular ion, followed by (pre)dissociation. Vertical transition energies to the lowest excited states are available from experimental work, whereas information about higher excited states is available from theory only. Excited states for H_2O^+ have been treated theoretically by several authors [43–47]. The calculated surfaces are expected to apply reasonably well also for HDO^+ . Recently, Schneider *et al.* [43] have performed an extensive study of C_{2v} potential-energy surfaces of the doublet states of H_2O^+ . Since the ground state is of C_{2v} symmetry, these calculations yield information about the positions of the excited states (also of C_{2v} symmetry) reachable by a vertical transition from the ground state. The full picture of possible dissociation pathways, however, must involve states of other symmetries. The observed peak around 5 eV can be explained by capture to a band of Rydberg states converging to the second excited state \tilde{B}^2B_2 of H_2O^+ (vertical transition energy 18.55 eV [48]). These Rydberg states are bound against dis-

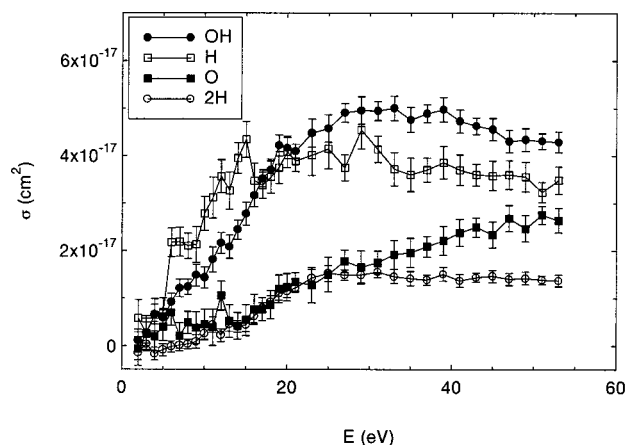


FIG. 4. Cross sections for DE of H_2O^+ as a function of energy. The error bars represent the uncertainty in the relative measurement. The cross sections are denoted according to the detector window in consideration; for instance, reactions leading to $\text{OH}+\text{H}^+$ and $\text{O}+\text{H}+\text{H}^+$ define the cross section labeled ‘‘OH.’’

sociation [43,46,47], but can be predissociated by other Rydberg states converging to higher-lying states of H_2O^+ as observed in electron-impact dissociation of H_2O [49]. Schneider *et al.* have calculated a number of ionic states with excitation energies around 9–20 eV. The corresponding Rydberg states may be responsible for the observed peak at ~ 15 eV.

B. DE cross sections

The measured cross sections for dissociative excitation of H_2O^+ as a function of energy are shown in Fig. 4. Except for the H channel, which exhibits a sharp rise at 5 eV, all cross sections rise relatively smoothly after threshold. The H and OH channels are seen to dominate the cross sections, indicating that the DE process preferentially breaks an OH bond leading to either $\text{H}+\text{OH}^+$ or H^++OH (or $\text{H}^++\text{O}+\text{H}$). At higher energies the O channel is of increasing importance. Besides a few structures, the DE cross sections are relatively smooth functions of energy. We observe a peak at ~ 12 eV in the O channel accompanied by a drop in the 2H channel, probably due to a resonant coupling to one of the excited states in the region 9–20 eV. Several structures appear in the H channel, which may be associated with electron capture to highly excited Rydberg states followed by autoionization to ionic states. The ionic states may be repulsive states or bound states that are predissociated. The calculations by Schneider *et al.* predict several states in the considered energy range [43].

In the case of HDO^+ , the DE cross sections for the OH and OD channels were measured (see Fig. 5). These cross sections reveal a significant isotope effect, with the branching ratio of the two channels being approximately 2:3 in the energy range with appreciable cross sections. The OH channel consists of DE events leading to $\text{OH}+\text{D}^+$ or $\text{O}+\text{H}+\text{D}^+$, and likewise for the OD channel. OH and OD bonds possess no significant differences in the electronic structure, and the observed isotope effect must therefore originate from the effect of the mass difference on the nuclear motion.

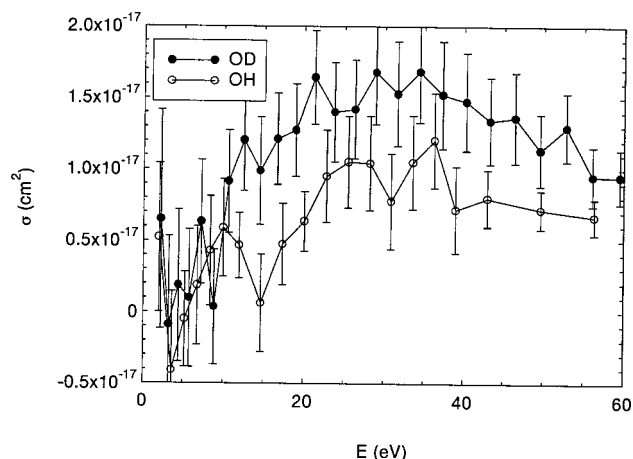


FIG. 5. The measured cross sections for DE of HDO^+ as a function of energy, error bars representing the uncertainty in the relative measurement.

C. DR branching ratios

Typical energy spectra from the surface barrier detector are shown in Fig. 2. Counts from each peak are extracted by fitting with Gaussian functions. The set of equations for H_2O^+ given in Eq. (8) are solved, yielding, in accordance with Eq. (10), the branching ratios for DR of H_2O^+ at $E=0$:

$$\begin{aligned} N_a(\text{OH}+\text{H}) &= 0.30 \pm 0.05, \\ N_b(\text{O}+\text{H}_2) &= 0.13 \pm 0.03, \\ N_c(\text{O}+\text{H}+\text{H}) &= 0.57 \pm 0.06. \end{aligned} \quad (13)$$

Three-particle breakup is the dominating process, taking about 57% of the flux. This process has been observed to be important also in the dissociative recombination of H_3O^+ [6,7] and CH_3^+ [7], and in H_3^+ [2–4]. Within the uncertainties, the results presented here are in agreement with our earlier results [7], but the uncertainties have now been reduced by more than a factor of 2. Branching ratios for dissociative recombination of H_2O^+ have also been measured in a flowing-afterglow experiment performed by Rowe *et al.*, who obtained $N_a(\text{OH}+\text{H})=0.55$, $N_b(\text{O}+\text{H}_2)<0.21$, and $N_c(\text{O}+\text{H}+\text{H})>0.24$ [13].

The following branching ratios are obtained for DR of HDO^+ at $E=0$:

$$\begin{aligned} N_{a1}(\text{OD}+\text{H}) &= 0.21 \pm 0.03, \\ N_{a2}(\text{OH}+\text{D}) &= 0.10 \pm 0.04, \\ N_b(\text{O}+\text{HD}) &= 0.10 \pm 0.04, \\ N_c(\text{O}+\text{H}+\text{D}) &= 0.59 \pm 0.07. \end{aligned} \quad (14)$$

The *b* and *c* channels for H_2O^+ are evidently not affected by the isotope substitution. The *a* channel in the H_2O^+ case ($\sim 30\%$) is shared by the corresponding channels, *a1* ($\sim 20\%$) and *a2* ($\sim 10\%$), in HDO^+ . This is in contrast to the results of the $\text{H}_3^+/\text{H}_2\text{D}^+$ experiment performed by Datz *et al.*, who observe that the three-particle breakup process is

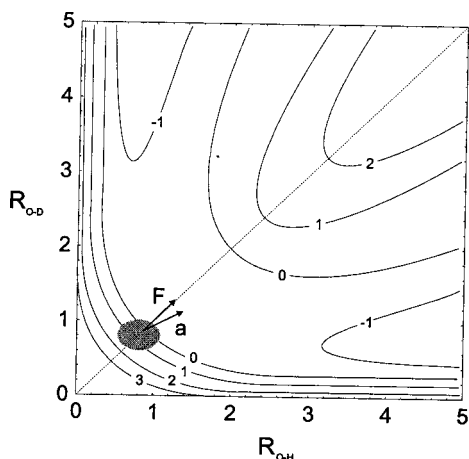


FIG. 6. Schematic model potential-energy surface for fixed HOD angle. Internuclear distances and energies of equipotential curves are given in arbitrary units. The gray ellipse depicts the nuclear wave function immediately after excitation.

more important in the DR of H_3^+ than in the DR of H_2D^+ [4,5]. The only significant isotope effect observed in the present DR measurements, is the 2:1 ratio between $N_{a1}(\text{OD}+\text{H})$ and $N_{a2}(\text{OH}+\text{D})$. This effect was also observed by Datz *et al.*, although in that case the isotope effect was not as pronounced as in the present experiment. After correcting for the statistical predominance of H, Datz *et al.* obtained a ratio of 1.2 between H release ($\text{HD}+\text{H}$) and D release (H_2+D).

A full explanation of the observed 2:1 ratio between $N_{a1}(\text{OD}+\text{H})$ and $N_{a2}(\text{OH}+\text{D})$ requires knowledge about the initial wave function and the potential-energy surfaces participating in the process. The shape and position of the nuclear wave packet formed after electron capture are determined by the Franck-Condon overlap between the initial ionic state and the repulsive neutral potential-energy surface on which the dissociation process takes place. This neutral potential-energy surface in turn determines the evolution of the wave packet. Since H and D are electronically equivalent, isotope effects can originate only from asymmetries in the nuclear motion caused by the mass difference of H and D. In the following, two kinematic effects which are independent of the potential-energy surfaces are discussed.

Consider capture into a repulsive potential-energy surface having the two possible dissociation pathways, $\text{OD}+\text{H}$ and $\text{OH}+\text{D}$. Since the two dissociation pathways are electronically equivalent, we focus on the nuclear dynamics, and in the present description the nuclear motion is restricted to the stretching degree of freedom. This approximation is only valid if the coupling between the stretching and bending degrees of freedom is relatively weak. Figure 6 depicts a model potential-energy surface of the type expected to account for the excited state in consideration. The gray ellipse illustrates the nuclear wave packet immediately after capture. It is centered around the $R_{\text{OH}}=R_{\text{OD}}$ line and has an elliptic shape, which will be the case if the ionic and neutral potential-energy surfaces intersect at the center of the initial nuclear wave function of the molecular ion. However, this aspect is not important for the present discussion. The force on the system is perpendicular to the equipotential curves. This does not apply for the acceleration, because of the mass dif-

ference between H and D. Let F_{OH} and F_{OD} denote the components of the force in the R_{OH} and R_{OD} directions, respectively. Then the force vector can be written as $\vec{F} = (F_{\text{OH}}, F_{\text{OD}})$. The corresponding acceleration vector is obtained from Newton's second law:

$$\vec{a} = \left(\frac{F_{\text{OH}}}{\mu_{\text{OH}}}, \frac{F_{\text{OD}}}{\mu_{\text{OD}}} \right), \quad (15)$$

where μ_{OH} and μ_{OD} are the reduced masses moving in the R_{OH} and R_{OD} directions. If both components F_{OH} and F_{OD} of a given force vector are nonzero, the corresponding acceleration vector will be rotated towards the $\text{OD}+\text{H}$ exit channel, since $\mu_{\text{OH}} < \mu_{\text{OD}}$. Consequently, this effect favors dissociation along the $\text{OD}+\text{H}$ pathway. The same effect is present in both resonant and nonresonant DE.

Proceeding along a dissociation pathway, the actual relaxation of the system must be considered. The newly formed neutral system relaxes by autoionization or dissociation. Independent of the exact shape of the repulsive potential-energy surface, the time a fragment needs to travel a certain distance scales as

$$t \propto \sqrt{\mu}. \quad (16)$$

Since autoionization is possible only within a confined region of space, the time needed for the fragments to leave this region is crucial. If the rate of autoionization does not depend strongly on the chosen dissociation pathway, the autoionization probability scales as $\sqrt{\mu}$. Thus, the effect of autoionization also favors the $a1$ channel compared to the $a2$ channel in the DR of HDO^+ . Resonant DE is subject to a similar effect.

The above discussion of kinematic effects does not take into account the details of the initial vibrational wave function of the molecular ion. This wave function is broader in the R_{OH} dimension than in the R_{OD} dimension, and hence isotope effects may arise if the capture process is sensitive to the tails of the wave function, i.e., if the intersection between the two potential surfaces (ionic and neutral) is at the edge of the initial vibrational wave function and not near the center as assumed in the discussion above. In such a situation, however, the cross section is likely to be small, which is obviously not the case for H_2O^+ and HDO^+ . The nodal structure of the initial vibrational wave function has not been considered here, since the present experiment has been performed on molecular ions in the vibrational ground state. However, results obtained from photodissociation of vibrationally excited HDO [25] and bimolecular reactions of vibrationally excited HDO with hydrogen atoms [34] indicate that vibrational preexcitation may have a strong influence also on the DR branching ratios.

In conclusion, isotope effects may be caused by several things, all resulting from the influence of the mass difference of H and D. Whereas the consequences of some of these effects cannot be determined without knowledge about the potential-energy surfaces, the two kinematic effects presented here unambiguously favor H release over D release.

IV. CONCLUSION

Absolute cross sections for dissociative recombination of H_2O^+ and HDO^+ have been measured as a function of energy. The relative cross sections for the two molecules closely resemble each other, only the absolute values may deviate somewhat. This is in contrast to the case of H_3^+ and HeH^+ and the corresponding isotopically substituted systems. The cross sections exhibit structures at low energy due to the opening of autoionization channels, and at high energy due to capture into highly excited Rydberg states.

Absolute cross sections for dissociative excitation of H_2O^+ and HDO^+ as a function of energy were also measured. In the HDO^+ case, an isotope effect favoring the OD channel over the OH channel is evident.

Branching ratios for dissociative recombination of H_2O^+ and HDO^+ at $E=0$ have been determined. The H_2O^+ results are more accurate than our earlier results. The corresponding branching ratios for dissociative recombination of HDO^+ reveal an isotope effect favoring H release. We have discussed two kinematic effects, which support this observation.

ACKNOWLEDGMENTS

This work has been supported by the Danish National Research Foundation through the Aarhus Center for Atomic Physics (ACAP). We thank the ASTRID staff for their assistance during the experiment.

-
- [1] A. Sternberg and A. Dalgarno, *Astrophys. J.* **99**, 565 (1995).
 [2] S. Datz *et al.*, *Phys. Rev. Lett.* **74**, 896 (1995).
 [3] S. Datz *et al.*, *Phys. Rev. Lett.* **74**, 4099 (1995).
 [4] S. Datz *et al.*, *Phys. Rev. A* **52**, 2901 (1995).
 [5] S. Datz *et al.*, in *Dissociative Recombination: Theory, Experiment and Applications III*, edited by D. Zajfman, J. B. A. Mitchell, D. Schwalm, and B. R. Rowe (World Scientific Publishing, Singapore, 1995), pp. 151–163.
 [6] L. H. Andersen *et al.*, *Phys. Rev. Lett.* **77**, 4891 (1996).
 [7] L. Vejby-Christensen *et al.*, *ApJ* **483**, 531 (1997).
 [8] Å. Larson *et al.*, *Astrophys. J.* **505**, 459 (1998).
 [9] J. Semaniak *et al.*, *Astrophys. J.* **498**, 886 (1998).
 [10] G. Herzberg, *Molecular Spectra and Molecular Structure I.—Spectra of Diatomic Molecules*, 2nd ed. (Krieger Publishing Company, Melbourne, FL, 1989).
 [11] G. Herzberg, *Molecular Spectra and Molecular Structure III.—Electronic Spectra and Electronic Structure of Polyatomic Molecules*, 2nd ed. (Krieger Publishing Company, Melbourne, FL, 1991).
 [12] P. M. Mul, J. Wm. McGowan, P. Defrance, and J. B. A. Mitchell, *J. Phys. B* **16**, 3099 (1983). This H_2O^+ cross section has been divided by a factor of 2 [J. B. A. Mitchell (private communication)].
 [13] B. R. Rowe *et al.*, *J. Chem. Phys.* **88**, 845 (1988).
 [14] D. R. Bates, *Astrophys. J.* **306**, L45 (1986).
 [15] D. R. Bates, *J. Phys. B* **24**, 3267 (1991).
 [16] E. Herbst, *Astrophys. J.* **222**, 508 (1978).
 [17] E. T. Galloway and E. Herbst, *Astrophys. J.* **376**, 531 (1991).
 [18] S. W. Englander, L. Mayne, Y. Bai, and T. R. Sosnick, *Protein Sci.* **6**, 1101 (1997).
 [19] T. Tanabe *et al.*, *Phys. Rev. A* **49**, R1531 (1994).
 [20] J. B. A. Mitchell *et al.*, *J. Phys. B* **17**, L909 (1984).
 [21] P. Van der Donk, F. B. Youssif, and J. B. A. Mitchell, *Phys. Rev. A* **43**, 5971 (1991).
 [22] H. Hus, F. Youssif, A. Sen, and J. B. A. Mitchell, *Phys. Rev. A* **38**, 658 (1988).
 [23] T. Tanabe *et al.*, in *Dissociative Recombination: Theory, Experiment and Applications III*, edited by D. Zajfman, J. B. A. Mitchell, D. Schwalm, and B. R. Rowe (World Scientific Publishing, Singapore, 1995), pp. 84–93.
 [24] N. Shafer, S. Satyapal, and R. Bersohn, *J. Chem. Phys.* **90**, 6807 (1989).
 [25] V. Engel and R. Schinke, *J. Chem. Phys.* **88**, 6831 (1988).
 [26] E. Segev and M. Shapiro, *J. Chem. Phys.* **77**, 5604 (1982).
 [27] R. L. Vander Wal, J. L. Scott, and F. F. Crim, *J. Chem. Phys.* **92**, 803 (1990).
 [28] R. L. Vander Wal *et al.*, *J. Chem. Phys.* **94**, 3548 (1991).
 [29] Y. Cohen, I. Bar, and S. Rosenwaks, *J. Chem. Phys.* **102**, 3612 (1995).
 [30] O. Atabek, M. T. Bourgeois, and M. Jacon, *J. Chem. Phys.* **87**, 5870 (1987).
 [31] T. Schröder, R. Schinke, M. Ehara, and K. Yamashita, *J. Chem. Phys.* **109**, 6641 (1998).
 [32] D. F. Plusquellic, O. Votava, and D. J. Nesbitt, *J. Chem. Phys.* **109**, 6631 (1998).
 [33] M. Brouard and S. R. Langford, *J. Chem. Phys.* **106**, 6354 (1997).
 [34] R. Metz, J. D. Thoemke, J. M. Pfeiffer, and F. F. Crim, *J. Chem. Phys.* **99**, 1744 (1993).
 [35] K. Furuya, F. Koba, and T. Ogawa, *J. Chem. Phys.* **106**, 1764 (1997).
 [36] P. J. Richardson, J. H. D. Eland, P. G. Fournier, and D. L. Cooper, *J. Chem. Phys.* **84**, 3189 (1986).
 [37] K. O. Nielsen, *Nucl. Instrum.* **1**, 289 (1957).
 [38] L. H. Andersen, J. Bolko, and P. Kvistgaard, *Phys. Rev. A* **41**, 1293 (1990).
 [39] L. Vejby-Christensen *et al.*, *Phys. Rev. A* **53**, 2371 (1996).
 [40] H. Danared *et al.*, *Phys. Rev. Lett.* **72**, 3775 (1994).
 [41] D. R. Bates, *Phys. Rev.* **78**, 492 (1950).
 [42] J. N. Bardsley and M. A. Biondi, *Adv. At. Mol. Phys.* **6**, 1 (1970).
 [43] F. Schneider, F. Di Giacomo, and F. A. Gianturco, *J. Chem. Phys.* **105**, 7560 (1996).
 [44] J. A. Smith, P. Jørgensen, and Y. Öhrn, *J. Chem. Phys.* **62**, 1285 (1975).
 [45] P. J. Fortune, B. J. Rosenberg, and A. C. Wahl, *J. Chem. Phys.* **65**, 2201 (1976).
 [46] G. G. Balint-Kurti and R. N. Yardley, *Chem. Phys. Lett.* **36**, 342 (1975).
 [47] R. A. Rouse, *J. Chem. Phys.* **64**, 1244 (1976).
 [48] C. R. Brundle and D. W. Turner, *Proc. R. Soc. London, Ser. A* **307**, 27 (1968).
 [49] J. Kurawaki, K. Ueki, M. Higo, and T. Ogawa, *J. Chem. Phys.* **78**, 3071 (1983).
 [50] B. Weis *et al.*, *J. Chem. Phys.* **91**, 2818 (1989).